Review Article

Metal oxide/chitosan composite for organic pollutants removal: A comprehensive review with bibliometric analysis

Khairunnas Ahmad[1]* and Williams Chiari[2]

[1]Department of Chemistry, Faculty of Mathematics and Natural Sciences, Universitas Syiah Kuala, Banda Aceh, Indonesia; [2]Department of Mathematics, Faculty of Mathematics and Natural Sciences, Universitas Syiah Kuala, Banda Aceh, Indonesia.

*Corresponding author: khairuna22@mhs.usk.ac.id

Abstract

Organic pollutants are now a global concern because of their rapid increase following the rapid industrial growth. In tackling this problem, researchers have used chitosan that could act as adsorbing material. However, chitosan use in wastewater treatment requires further modification owing to its drawbacks of being susceptible to acidic environment and mechanically weak. Of many modifying approaches, metal-oxide embedment is perceived as promising because not only does it improve the chemical and physical properties of chitosan, but it also adds new features to the material such as being magnetic or photocatalytic. This present review describes the modification of chitosan through metal oxide embedment aiming to its utility in organic waste removal. Firstly, the definition of chitosan and the progress of its application in wastewater treatment are presented. Types of metal oxides, namely photocatalyst and magnetic iron oxide are also discussed. Embedment of metal oxides into chitosan could be done using methods such as sol-gel, high-energy ball milling, and spray-drying, where they affect the chemical and physical properties of the produced metal oxide/chitosan composites. Reported studies suggest a high percentage of organic pollutant removal, up to 100%. In addition to its removal ability, metal oxide/chitosan is also proven to be environmentally friendly and economical.

Keywords: Chitosan, metal oxide, organic pollutant, human health, wastewater

Introduction

Degradation of the environmental quality from organic and inorganic waste has been a widespread challenge, especially for water resources. Some of the pollutants are accumulated in the water that surpass the safe limit [1]. Organic pollutants can come from the natural environment and biological processing [2], to various industries that are increasing rapidly, such as agriculture [3] and textile industries [4]. Some of these organic pollutants include pharmaceutical waste, pesticides, dyes, and common organic chemicals. These organic pollutants are highly toxic and capable of affecting human health, either through direct contact, or indirectly through contamination of the food chain. In addition, organic pollution is not only resulting a high risk in human health, but also harmful for the ecosystem [5]. Therefore, the removal of such a pollutant from the water is crucial for both environment and human health [6].

Several methods to remove these pollution have been investigated, including evaporation, freezing, ion exchange [7], and adsorption using membrane such as chitosan [8]. Chitosan-based materials are used due to their benefits, including less toxic, biodegradability, and efficient

Received: April 4, 2023 - Accepted: August 21, 2023 - Published online: August 31, 2023

adsorption ability [9]. Some sources of raw material for chitosan preparation are shrimp and crab shell [10]. However, chitosan has a drawback on low capacity for organic removal. Therefore, embedding the biopolymer with fillers are needed to complement its shortcomings.

Recently, photocatalyst materials have attracted the attention from researchers due to their advantages for organic pollution removal. Photocatalysts are popularly derived from metal oxides, such as TiO_2 [11], Fe_2O_3 , and ZnO [12]. The photocatalysis method becomes stand out among others because it did not produce secondary pollutants after the treatment. By using a photocatalyst, the substrate absorbs light energy that causes the formation of excited electron (e^-) and a positive hole (h^+) leading to the reduction and oxidation which catalyzes the degradation of the contaminants [13]. Embedment of these metal oxides onto polymeric matrix has been reported to prevent their aggregation, thereby increasing contact surface and subsequently removal efficiency. This review article will discuss recent advances of metal oxide/chitosan composites and focus on their application in removing organic pollutants from wastewater.

Chitosan

Chitosan: Source and modification

Chitosan-based adsorbents are widely used to remove various contaminants owing to economical convenience, ease of preparation, reusability, biodegradability, and high adsorption capacity (due to functional groups that act as binding sites) [14]. Chitosan is a biopolymer that can be synthesized from various living organisms [15], some of widely utilized source include shrimp and crab shells [10]. In addition, lobster, crayfish and oyster have also been reported as the source of chitosan [16,17]. Reported sources and methods for preparing chitosan are presented in **Table 1**. Ultrasound, microwave, and thermal treatments are commonly used as physical methods for chitosan preparation. They are fast, easy or straightforward, and efficient, and produce high yield of acid-soluble chitosan with stable chemical and thermal properties [18]. The process includes soaking the raw material into NaOH solution with high temperature condition for few hours that resulting on a high chitosan that soluble in acidic medium [19]. The presence of NaOH in microwave irradiation method for 2 h at 350 W is considered as fast and efficient method [20]. As supported by other research that shows both alternate irradiation in the presence of NaOH [21] and ultrasound-assisted deacetylation of chitin [22] resulting on a high yield of chitosan with acid-soluble properties. In addition, the deacetylation of chitosan in NaOH solution under 600-W microwave irradiation improves the antimicrobial activity of chitosan [23]. The UV irradiation method at different interval of time improves the flame-retardant property of chitosan [24]. Meanwhile, the modified chitosan using GDP method produced a chitosan with several advantages, including high thermal stability, tensile strength, and vapor barrier [25]. A simple ball milling, in combination with thermal shocking drying, can be employed to produce nano-chitosan (diameter <30 nm) [26]. Chitosan with high mechanical and thermal properties can be achieved by hot press method [27].

Chitosan for wastewater treatment: Advantages and disadvantages

The application of chitosan for wastewater treatment has been reported widely due to their several advantages. Chitosan has a number of favorable properties, such as nontoxic, antibacterial, biodegradable, and biocompatible [30], which makes it an effective adsorbent material for removing wastewater pollutants. Compared to other polysaccharides, such as starch and galactomannan, the structure of chitosan allows for some controlled specific modifications, which is an important advantage. Moreover, the amino and hydroxyl groups on the chitosan backbone show the application of a large chitosan adsorbent for wastewater treatment [31].

Despite all the advantages mentioned above, several disadvantages of chitosan limit its application, unless modified as composite. One of main disadvantages of chitosan is insoluble in water [32]. This drawback of chitosan because of the crystalline structure that formed by strong hydrogen bonding between hydroxyl and carbonyl and acetamide group that inhibit water-soluble chitosan [33]. Therefore, changing the structure of chitosan will improve their solubility ability in water, as reported, modification using carboxymethyl improve the ability water without

changing other crucial characteristics [34]. Not only insoluble in water, pure chitosan also has other disadvantages, including weak in mechanical strength, less resistant to acid, and low recycle ability [35]. As answer for this disadvantages, several effort have been reported, such chemical cross-linking or blending chitosan with others polymers, including cellulose, polyacrylamide, and polyvinyl alcohol (PVA)[36] .

Table 1. Sources of raw materials and methods used for chitosan preparation

Ref	Source	Method	Preparation condition	Advantage
[18,19,28]	*Penaeus kerathurus*, *Carcinus mediterraneus*, *Sepia officinalis*	Chemical	12.5 NaOH (140°C for 4 h), soaking in 18 M NaOH (24 h), heating (90°C for 7 h)	Soluble in acidic medium
[20]	*Penaeus kerathurus*	Microwave radiaton	50 % NaOH, 8 min irradiation at 350 W	Fast, easy, and efficient
[21]	*Macrobrachium rosenbergii*	Ultrasound irradiation	40 % NaOH, alternate irradiation (45 min), Ultrasound-assisted deacetylation chitin in 40 % NaOH (50 min, 60°C) irradiation	High yield of acid-soluble chitosan
[24, 29]	*Penaeus kerathurus*	UV irradiation	Exposure UV/ ozone at different time intervals	Improve flame retardant properties
[23]	*Litopenaeus vannamei*	Chemical and microwave	Deacetylation in NaOH solution under microwave irradiation at 600 W	High antimicrobial activity
[25]	Conventional	Glow discharge plasma	GDP of 0–800 W for 1 min	High thermal stability, tensile strength, WV
[26]	*Penaeus kerathurus*	Milling	Solubilized mixture of HAc and NaOAc, autoclave 121°C at 1 atm for 5 min, thermal shock drying	Nanochitosan diameter <30 nm, Mv<21 kDa
[27]	*Macrobrachium rosenbergii*	Hot press method	PLA-laminated chitosan by hot pressing	Mechanical and thermal properties

Metal oxide

Photocatalyst

Photocatalysis refers to the combination of photon (light) and catalyst and is the properties mostly found in semiconductor materials such as metal oxides [37]. In wastewater treatment photocatalytic reaction includes the organic pollutant degradation, heavy metal ion oxidation–reduction transformation, and the reduction of carbon dioxide (CO_2) [38]. The schematic diagram summarizes the photocatalytic reaction is presented in **Figure 1**.

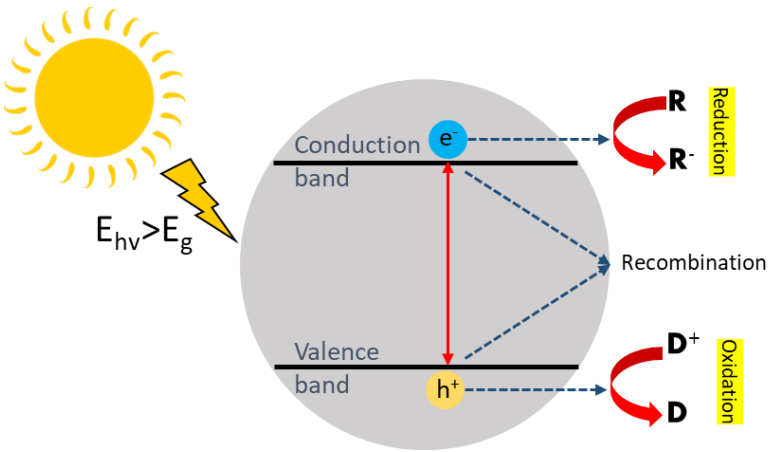

Figure 1. Photocatalysis reaction mechanism, as adopted from [41].

Photocatalysis process occurs when a light irradiates a photocatalyst. When the light energy is larger than the photocatalyst bandgap energy, the light absorbed and triggers charge separation, which causes the electron (e^-) excitation from valence band to conduction band [39]. Hole (h^+) then is left in valence band [39]. Afterward, the resultant e^- in the conduction band and the h^+ in the valence band move to the photocatalyst surface. The quantum yield will be reduced due to the e^- and h^- recombination, which is influenced by many photocatalyst structures and surface modifications related factors [40]. The reactive e^- and h^+ on photocatalyst surface facilitate reduction and oxidation reactions, respectively, resulting in an excess of Reactive Oxygen Species (ROS), such as superoxide anion (O_2•) and radical hydroxyl (•OH). Water molecules can be oxidized by the h^+ to form radical hydroxyl, while the radical group subsequently oxidizes organic pollutant in the wastewater [41].

Magnetic iron oxide

Magnetic iron oxide is Magnetic metal oxide is a magnetically strong metal derivative. It has a wide range of uses for various technological applications, from magnetic media recording to photochemical catalysts. Magnetic metal oxides have a cube crystal structure that comes in various shapes and sizes [42]. The crystal structure differs depending on the type of metal used, for example $NiFe_2O_4$ has a spinel structure [43], and $MnFe_2O_4$ has a cube structure [44]. Each structure has a different density, magnetization, and coercivity.

Magnetic oxides can be synthesized in various ways, including thermal decomposition, hydrothermal synthesis, and coprecipitation [45]. It can also be synthesized from metal-containing compounds, such as chlorides, nitrates, and sulfates. In addition, it can be produced from metal ores by heating them with carbon. Metal magnetic oxides have many industrial uses [46], such as making tape recordings, coatings, and polishing components and are used in water treatment and biomedicine.

Metal magnetic oxides have many benefits as photocatalysts. Due to their strong magnetic properties, they are ideal for use in magnetic separation processes. In addition, it is effectively used for the decomposition of organic pollutants, as it has excellent catalytic properties for the oxidation of organic compounds. Its magnetic properties also make it useful for improving the efficiency of some photocatalytic processes [47]. For example, it can be used to increase the photocatalytic reaction rate by increasing the intensity of absorbed light and increasing the reaction exposure time. In addition, its high stability makes it ideal for use in photocatalytic reactions that require high temperatures. Finally, it can be used as a catalyst for the production of hydrogen and oxygen from water. This process, known as water splitting, is an important part of energy production and storage. Metal magnetic oxides are promising catalysts for water splitting due to their favorable magnetic and catalytic properties.

Metal oxide/chitosan

Preparation

The synthesis of metal oxide/chitosan requires a number of steps, including the selection of metal oxide, chitosan, surfactant, and the method to be used to obtain the desired composite. This section will provide brief information on the methods used for metal oxide/chitosan synthesis.

Sol-gel method

The sol-gel method is widely used for composites preparation. The stages of this method begin with the preparation of a solution of metal oxides and chitosan. Then, a series of chemical reactions are carried out to form a gel. In this method, metal oxides must be in their salt form and chitosan must be in molecular form. The solution is then stirred at the right temperature for 1–2 h to ensure complete dissolution of metal oxides and chitosan. Once the solution is cooled, an acid or base is added to set the pH between 3.0 and 4.0 to prevent the precipitation of metal ions. The mixture is then allowed to stand for 24 h before filtered to remove any undissolved particles.

High-energy ball milling

In this method, a mixture of metal oxides and chitosan is added with surfactants. The mixture is then grinded with high-energy mechanics. The grinding process using ball mill is carried out to

break metal oxides into particles with smaller sizes. Surfactants are used to help keep the distribution of parties in composites uniform. Grinding is carried out in dry conditions to prevent composites from getting wet and sticking together.

Spray-drying

This method is performed by spraying a solution of metal oxide/chitosan in a drying chamber, where the solution can be evaporated quickly. This drying process involves the use of a nozzle that has a high pressure. Rapid evaporation of the solution will prevent the forming of desired composite. Afterward, composite can then be obtained and collected from the drying chamber.

Characteristics

FT-IR

Chitosan is comprised of O- and N-containing functional groups deriving from O–H, N–H, C=O, and C–O–H moieties which contribute to the contaminant uptake by acting as active sites of the adsorbent. As metal oxide contains M–O bonding which can vibrate when irradiated by infrared with a certain wavenumber, the addition of this particle could ideally add new spectral peaks. For example, chitosan matrix filled with ZnO would have the spectral peaks observable at around 400 and 500 cm^{-1} corresponding to the stretching vibration of O–Zn–O [6,48,49]. Shifted wavenumber or changed intensity is often reported and associated with the interaction of matrix (chitosan) and metal oxide fillers. Changes on the FT-IR profile following the incorporation of metal oxides have been presented in **Table 2**.

Table 2. FT-IR Characterization result of metal oxide/chitosan

Ref	Filler	Moiety	Wavenumber (cm^{-1})	Remarks
[48]	ZnO	O–Zn–O	451	New
			436	New
		O–H	3423	Shifted
[6]	ZnO	O–Zn–O	524	New
			466	New
		Zn–O–Ce	564	New
		O–H	xxx	Increased
[51]	Zn, Mg	C–N–Metal	1377	New
[52]	CuO, CeO_2, Al_2O_3, Fe_2O_3	Al–O	1075	New
		Fe–O	425	New
		Ce–O	959	New
		CuO–CeO2–Al_2O_3	873	New
		CuO–CeO2–Fe_2O_3	873	New
[49]	ZnO	Zn–O	445	New
		O–H	3148	Shifted
		N–H	3289	Shifted
[53]	$ZnFe_2O_4$, CuO, $NiFe_2O_4$, Co_2O_3, Fe_3O_4, $FeCr_2O_4$	Fe–O	585	New
		Cu–O	420	New
		Ni–O	451	New
		Cr–O	469	New
		Zn–O	450	New
		Co–O	446	New
		R–O–R	1018	New
[54]	Fe-Al-Mn	Fe–O	580	New
		Al–O	650	New
		Mn–O	1013	New
[55]	FeO	Fe–O	699	New
			890	New

However, a study found the addition of CuO and ZnO did not add any new spectral peaks or result in shifted wavenumber [50]. The author argued that the absence of changes in the FT-IR spectra suggests no meaningful alteration on the functional groups, hence their performance as adsorbent active sites [50]. However, we should put critical note on the study, as the XRD characteristics also suggested the absence of significant effect of the metal oxide addition. Hence, the conclusion of the foregoing study should be taken with caution, where more investigations required to confirm the claims.

Morphology

Chitosan morphologies, based on SEM images, have been reported different from one another, starting from a round particle shape [6] up to the one with a plate-like geometry [53], depending on the shape of the material (such as film, beads, powder, etc.) prepared. Addition of nanoparticle often contribute to rough surface with observable metal oxide particles distributed around the material surface [6,52,53]. Decoration of metal oxide particles onto chitosan nanoparticles has been observed to add the particle size [49]. On contrary, reduced diameter has been observed in chitosan-coated iron oxide nanoparticles attributed to the confinement effect from chitosan allowing more compact particle density [55]. Agglomeration was found on the filler particles responsible for irregular size and shape of fillers [6,52]. Agglomeration of the nanoparticle could lower the contaminant uptake as it blocks the adsorbate reaching the active sites. Nonetheless, it should be noted that embedment on chitosan surface may serve as a agglomeration preventive strategy [54]. Moreover, benefits of improved chitosan bulk porosity from metal oxide embedment have been reported [50, 54]. A study confirmed the irregularity of the filler size and shape by using transmission electron microscope (TEM) [52]. Images from TEM could confirm the even distribution of the metal oxide particle in the matrix [54]. It is a common finding that the metal oxide is coated with the chitosan layer and consequently forms rugged surface [49,53]. An interesting presentation has been reported by a study using electrospun chitosan fibers as a matrix for flower-like shaped CaCOx nanoparticles (**Figure 2**) [56].

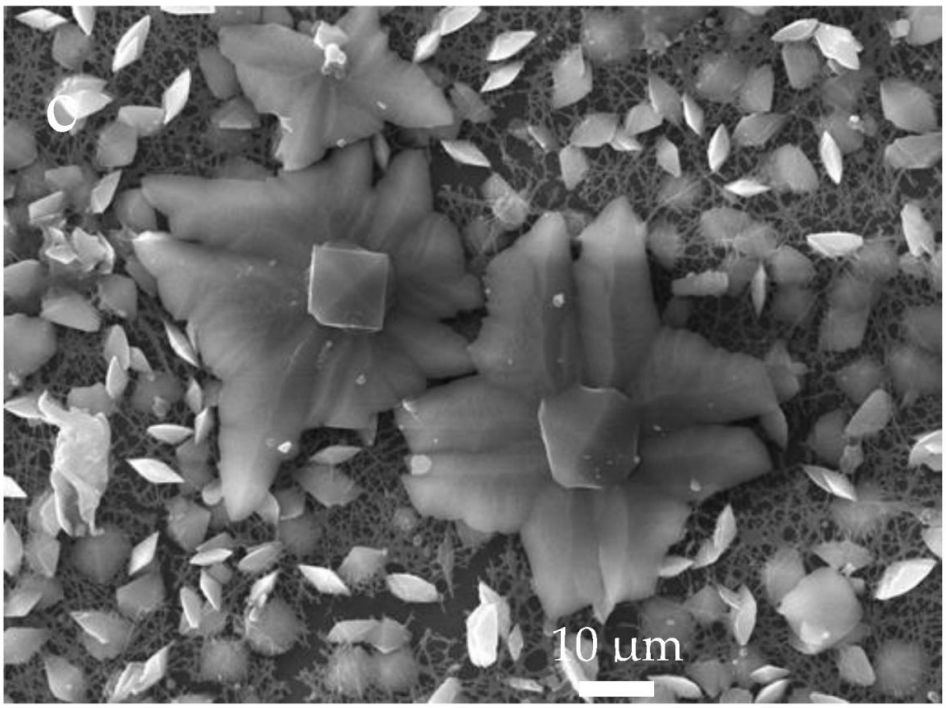

Figure 2. SEM images showing flower-like shaped fillers of metal oxide ($CaCO_x$) embedded onto fibrous chitosan matrix. Reproduced under the terms of Creative Commons Attribution (CC BY 4.0), citing [56].

Crystallinity

Diffraction peaks of chitosan are typically broad and usually generated at 2θ=11° and 20° owing to its semicrystalline nature [52]. The presence of metal oxide on the matrix would consequently result in new crystalline peaks. For example, crystalline peaks at 31.72°, 34.44°, 36.21°, and 56.6° have been assigned to the presence of ZnO which correspond to (100), (002), (101), and (110) crystallographic planes, respectively [6]. Diffraction profile of each nanoparticle could be differed based on its size, where smaller particle size tends to have noises [52]. There is not much similarity among the reported studies regarding the effect of metal oxide embedment toward the crystallinity of chitosan matrix. Decreased crystallinity, as suggested by the reduced intensity, has been observed after the incorporation of ZnO [50]. However, some other studies found that the crystallinity of the composite increased following the embedment of metal oxide, particularly ZnO

[49,53]. The ability of ZnO or its Zn forming a complex bonding with chitosan has been highlighted by several published reports [49,53]. Shifted diffraction angles have been proposed as another indication of the altered crystalline structure by metal oxides [49,50,53].

Thermal stability

In most studies, thermal degradation of chitosan profile consisted of water evaporation (around 100°C) and chitosan decomposition (around >400°C) [50]. There is a tendency of (thermal gravimetry analysis) TGA peaks to shift into lower temperatures after the addition of metal oxide, suggesting the disrupted integrity of chitosan intramolecular interactions [50]. Nonetheless, another study confirming the complexation of chitosan—ZnO nanoparticles suggested that the metal oxide contributed to higher thermal stability evidenced by decomposition onset at higher temperatures [49]. Similarly, a study employing inorganic oxyhydroxides to modify chitosan adsorbent also suggested an improved thermal property based on TGA thermogram [54]. In high temperatures, the metal oxide could undergo dihydroxylation resulting in mass loss, where coating with chitosan could improve its thermal stability [55].

Application in wastewater treatment

Photocatalyst

The data of chitosan performance for removing organic contaminants in wastewater using metal oxide have been provided in **Table 3**. Generally, chitosan with metal oxide support has been shown to have a high removal percentage of organic pollutants in wastewater, including antibiotics waste, natural chemical, and dye waste. This high removal performance can be obtained due to the photocatalytic activity of metal oxide that maximize the adsorption capability of composite [57]. The application of chitosan/metal oxide for dye waste and antibiotic waste removal shown the highest value at 100% for Methyl Orange (MO) [58] Malachite Green(MG) [6], Disperse Red 60 [52] and Ampicillin [58].

Table 3. Performance of chitosan for organic pollutant removal with metal oxide supports

Ref	Metal oxide	Pollutant (removal, %)	Optimum operating parameter(s)
[53]	$ZnFe_2O_4$	ANTH (95%); PHEN (92 %)	pH 7, 25 h
	$CuO-Fe_2O_3$	ANTH (93%); PHEN (90%)	
	$NiFe_2O_4$	ANTH (90%); PHEN (88%)	
	$Co_2O_3-Fe_3O_4$	ANTH (88%); PHEN (85%)	
	$FeCr_2O_4$	ANTH (83%); PHEN (81 %)	
[49]	ZnO	MB (96.7%)	pH 9, 1 h
[52]	$CuO-CeO_2-Al_2O_3$ (NCCA)	DR (100%)	pH 4
	$CuO-CeO_2-Fe_2O_3$ (NCCF)	DR (77%)	pH 2
[51]	Zn–Mg bimetal oxide	MO (74.05%)	pH 3, 2 h
		MB (67.43%)	pH 8, 2 h
[58]	Ag_2O/TiO_2	AMP (100%)	3 h
		MO (100%)	30 min
[6]	ZnO	MG (100%)	4.5 h
[61]	TiO_2	DV51 (95.63%)	1.5 h
[62]	CuO	99%	1 h
[63]	Fe_2O_3	RO (96%);	27°C, pH 7, 50 min
		MB (98%)	
[64]	GO	RB (96.2%)	25°C, pH 6, 40 h
[60]	GO-hydroxyapatite	CR (>65%);	pH 2, 40 min
		AR1 (>65%);	
		RR2 (>65%);	
[65]	GO	MB (90%)	pH 5.3, 1 h
[66]	ZnO	RB5 (76%)	pH 4, 6 h
[59]	GO	NR (60%)	pH 5
		RB (60%)	pH 4
[67]	ZnO	RBHN (95-99%);	50°C, 1 h
		RMHB (95-99%)	

DR: disperse red 60; MB: methylene blue; RBHN: Reactive Black HN; RB-5: Reactive Black 5; RMHB: Reactive Magenta HB; RB: Remazol Black; NR: Neutral Red; AR1: Acid Red 1; RR2: Reactive Red 2; CR: Congo Red; DV51: Direct Violet 51; MG: Malachite Green; AMP: Ampicillin; ANTH: Anthracene; PHEN: Phenanthrene; RO: Reactive Orange 16.

The removal for both MO and Ampicillin is using Ag_2O/TiO_2-modifed chitosan-based photocatalytic (ATCPF). The highest removal percentage is reached after 3 hours of degradation under solar irradiation. This high removal percentage is reached due to the heterostructure of Ag_2O/TiO_2 that is capable to expose and induce photocatalytic oxidation reaction into the ampicillin and MO solution. Similar to the removal of Malachite Green (MG) that reached 100% as well after 3 hours solar irradiation, using chitosan/ZnO composite. On the other hand, the removal of Disperse Red 60 was also reached at 100% using the support of $CuO–CeO_2–Al_2O_3$, after 4 hours of solar irradiation. The lowest percent removal shown for methyl orange (MO) [51], Remazol Black (RB), and Neutral Red (NR) [59], Congo Red (CR), Acid Red 1 (AR1) and Reactive Red 2 (RR2) [60] at 67.43%, 60% and 65% respectively using Zn–Mg bimetal oxide, GO, and GO–hydroxyapatite.

Magnetic

Metal oxide/chitosan composites have good magnetic properties, as metal oxide materials such as Fe_2O_3, $CoFe_2O_4$, and $NiFe_2O_4$ are incorporated into the chitosan matrix [68]. Metal oxide/chitosan composites have superparamagnetic properties, which means they have paramagnetic properties in the absence of an external magnetic field. However, it becomes magnetic when exposed to a magnetic field.

A study reported the synthesis of Fe_3O_4/chitosan nanocomposites and their magnetic properties. The study found that the composites exhibited super-paramagnetism, with a high saturation magnetization value of 54.1 emu/g [69]. The authors concluded that these composites have potential applications for future surface plasmon resonance (SPR)-based sensor applications. Another study reported the synthesis of Fe_3O_4–chitosan as a polymeric shell. Magnetic measurement revealed that the saturated magnetization of the Fe_3O_4–chitosan nanoparticles reached 21.5 emu/g and the nanoparticles showed the characteristics of super-paramagnetic [70].

There are many factors that affect the magnetic properties of metal oxide/chitosan composites, such as the synthesis method, and the type of metal used. The improvement in the properties of these composites is not only in their magnetic properties, but also in their stability and biocompatibility. Thus, metal oxide/chitosan composites are promising for use in various applications, one of which is wastewater treatment.

Reusability

Numerous research has reported that the application of metal oxide/chitosan composites shows a good ability to remove water pollutants, including organic substances and dyes. However, one important aspect that must be considered is the cost involved in its application. Therefore, the reusability of metal oxide/chitosan composites must be considered.

A study shows that CuO/Chitosan was able to degrade 99% of Rhodamine B (RhB) dye within 60 minutes when exposed to visible light. In addition to RhB dye, the researchers also tested the composite's ability to degrade crystal violet and Congo red dye under UV light irradiation. In both cases, almost 99% of the dye was effectively degraded through photocatalysis. Furthermore, the study found that the composite was reusable for up to five catalytic cycles [71]. Similar reusability of metal oxide/chitosan has been reported, using iron oxide/chitosan immobilized manganese peroxidase and its application for decolorization of textile wastewater [63]. The result show that reusability for the removal of methylene blue and reactive orange 16 was studied for successive five cycles [63].

Treatment system

Batch system

The use of a batch system involves adding a fixed amount of composite to the wastewater and allowing the adsorption process to take place over a period of time. Once the adsorption process has been completed, the composite is then removed, and the water that has been obtained is separated from the composite. The composite can then be reused until its ability reaches its minimum limit. The use of a batch system is relatively simple because it uses little equipment. Hence, this system is suitable for small-scale applications.

A study was conducted to create a hydrogel nano polymer by combining graphene oxide, chitosan, and PVA. The resulting material was tested for its ability to remove Congo red dye from a solution using a batch system. The researchers evaluated the concentration of dye left in the solution after the experiment and how much of the adsorbent material was able to remove the dye. When the pH was at 2, using 6g/L of adsorbent at a rotation speed of 140 rpm, 88.17% of the Congo red dye was removed when the initial concentration of dye in the solution was 20 mg/L. At a neutral pH, the efficiency of dye removal was around 81% [72].

A higher dye waste removal was reported by using the batch system. The research synthesized chitosan-graphene oxide hydrogels with embedded magnetic iron oxide nanoparticles and evaluated its application for methylene blue (MB). This research also evaluates the effect of adsorbent dosage, initial dye concentration, contact time, pH, and ionic strength. The result shows that the pH level and the ionic strength of the solution had a significant impact on how well the adsorption process worked. This suggests that the adsorbent and MB molecules interacted with each other due to electrostatic forces. The composite was able to quickly remove MB, with a rate constant of 0.06 g mg^{-1} min^{-1}. The hydrogel nanocomposites were tested over multiple cycles and showed excellent adsorption performance across different pH levels. The highest removal percentage of MB was achieved at pH 11 with an adsorbent dosage of 0.6 mg/mL, resulting in a 99.7% removal rate and an adsorption capacity of 36.2 mg/g [73].

Continuous flow system

Columns packed with composites are used in continuous flow systems, then wastewater is flow constantly through the columns. Thus, the adsorption process will occur continuously until the wastewater stops flowing through the column. Furthermore, once the adsorption process is complete, the treated water is collected at the bottom of the column, while the composite remains inside the column. The composite can then be reused for up to several cycles until it reaches its capacity limit. Although it will require more complex and expensive equipment for this system, the treatment capacity is higher, making it suitable for large-scale use [74].

A study was conducted to synthesize graphene oxide/chitosan sponge and its application in removing methylene blue using continuous flow system [75]. Adsorption efficiency increased as pH increased from 4 to 8. The flow rate was increased from 3.2 to 32mm/min, as the surface loading rate increased, while the adsorption capacity decrease. The reusability shows 4 cycles of adsorption-desorption with a slow decrease in adsorption capacity up to the 4^{th} cycle where it remained constant, with removal efficiency of >80% [76].

Another study used the same treatment, to remove Doxycycline (antibiotic) using Magnetic Fe_3O_4@chitosan carbon microbeads [77]. The results showed that the adsorption capacity increased as the pH value increased, from 2 to 11. When the initial concentration increased from 20 to 30 mg/L, the adsorption capacity decreased. When the flow rate increased from 1.1 to 3.1 mL/min, the adsorption capacity decreased with maximum absorption at 3.432 mg/g. Reusability showed 3 adsorption-desorption cycles and regeneration efficiency was above 80% in the first two cycles then decreased thereafter.

Bibliometric research trend

To evaluate the research trend of metal oxide/chitosan for wastewater treatment, we performed a bibliometric analysis using the data from the Scopus database. We used the following keyword combinations: 'Chitosan' AND ('Metal Oxide' OR 'ZnO' OR 'Fe_2O_3' OR 'FeO' OR 'magnetic' OR 'NiO' OR 'CuO' OR 'MgO' OR 'CrO' or 'MnO' OR 'CaO' OR 'Al_2O_3' OR 'AlO' OR 'TiO_2' OR 'SnO_2') AND ('Contaminant*' OR 'Pollut*' OR 'Wastewater' OR 'dye' OR 'effluent') AND NOT 'heavy metal'. Visualizations of the keywords co-occurrence and co-authorship countries were performed on Vosviewer 1.6.17 (Center for Science and Technology Studies, Leiden University, The Netherlands) on the co-occurring keywords and co-authorship countries [78]. The network visualizations of the keywords co-occurrences are presented in **Figure 3**. The largest research themes created their own cluster which were represented by the following keywords: 'chitosan', 'adsorption', 'regeneration', 'magnetic chitosan' and 'photocatalysis'.

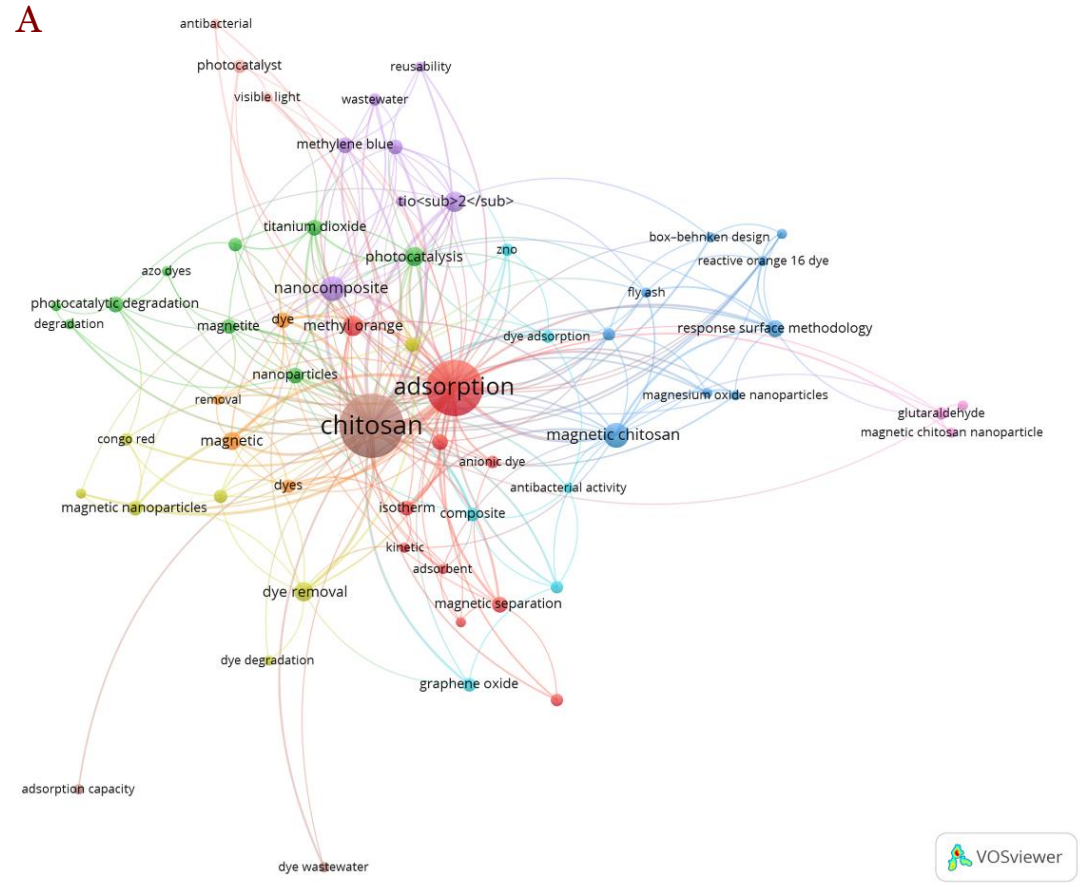

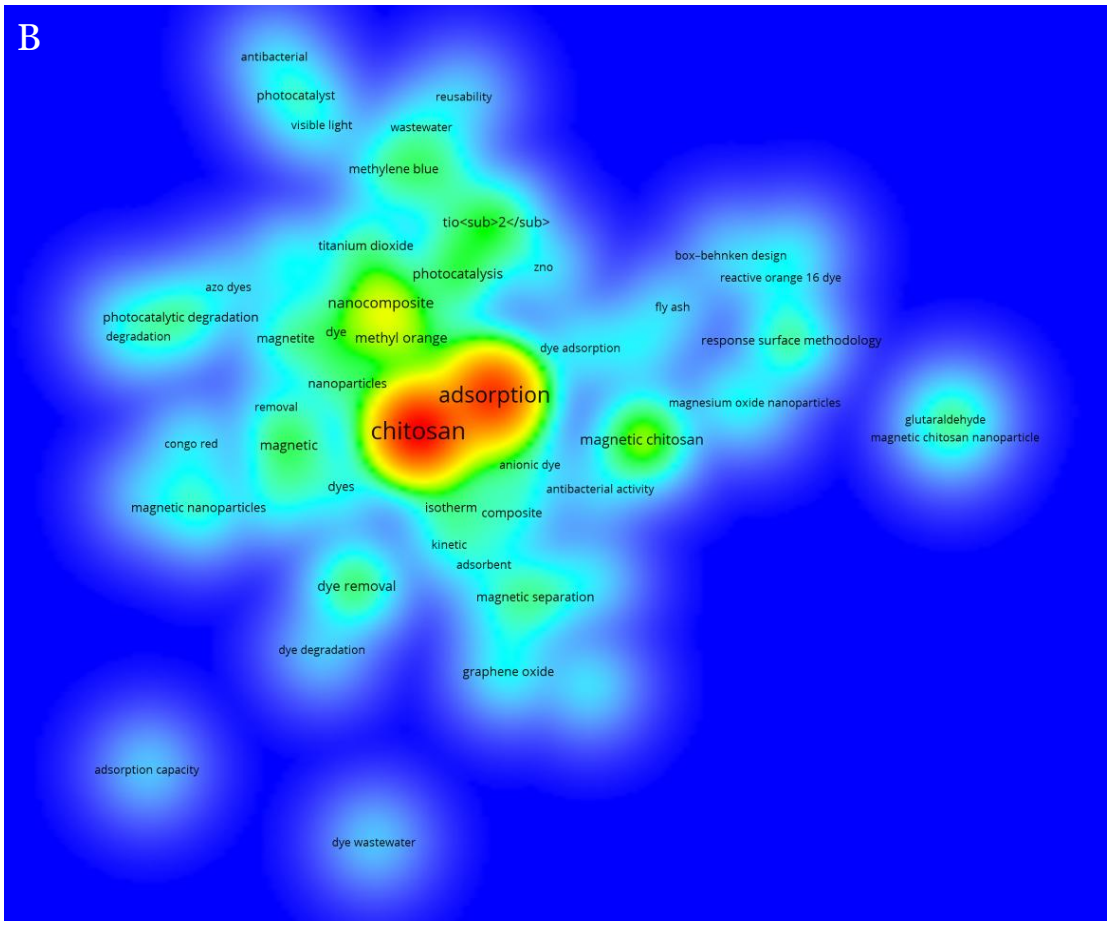

Figure 3. Network visualization (A) and density visualization (B) of keywords co-occurrence on research investigating metal oxide/chitosan for wastewater treatment.

The density visualization also shows the tendencies of certain keywords to the research study. The keyword in red represented the keywords with the highest density, followed by yellow, green and blue. This visualization shows that 'chitosan' and 'adsorption' were the keyword with the highest density, with some other keywords revolving around 'magnetic chitosan', 'nanocomposite', and 'magnetic separation'. The network visualization and density visualization maps for the co-authorship countries on chitosan and its application for environmental pollutant research have been presented in **Figure 4**. For the same purpose as the keyword co-occurrences analysis, restriction was imposed on the mappings, where a maximum of 25 countries per document and a minimum of 5 documents a country were set. Of 53 countries, 17 met the threshold and the analysis was represented by the mappings above.

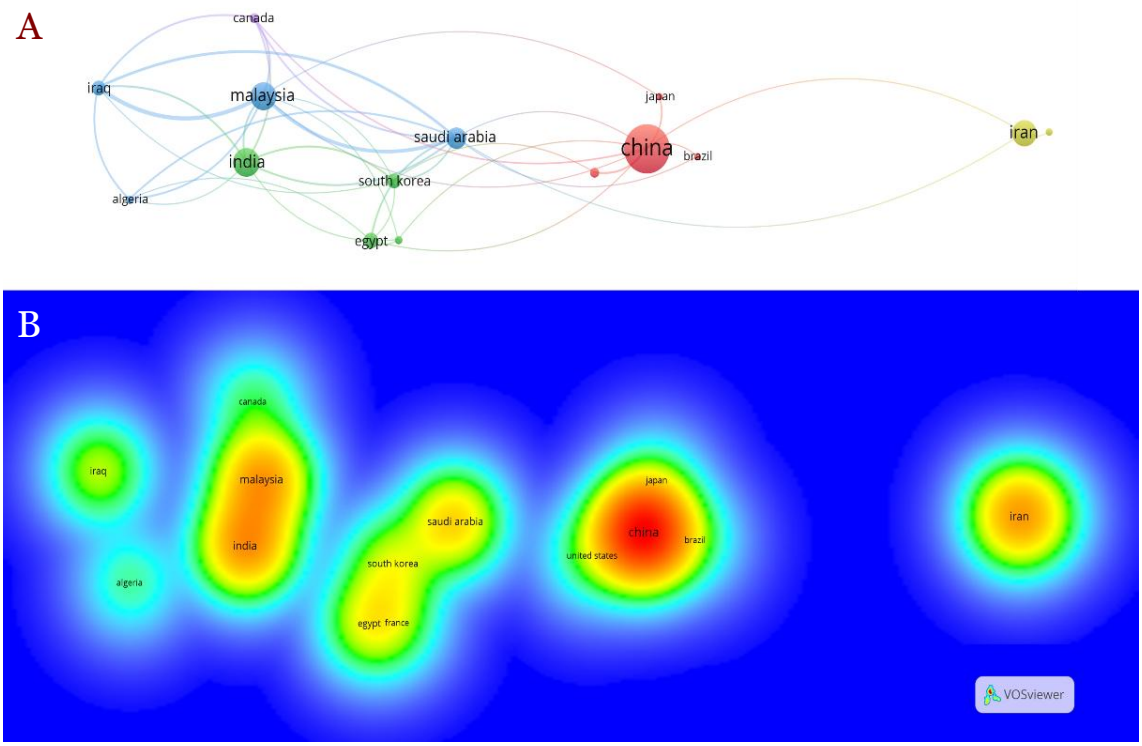

Figure 4. Network visualization (A) and density visualization (B) of co-authorship countries on research investigating metal oxide/chitosan for wastewater treatment.

China is the most productive country (documents=71, citations=3911, TLS=13), followed by Malaysia (documents=31, citations=1550, TLS=37), South Korea (documents = 13, citations = 1397, TLS=9) and South Korea (documents=22, citations = 1042, TLS=33). In other bibliometric analysis study, China was also revealed as the leading country in wastewater treatment or polymer research [79–81]. It is worth mentioning that despite publishing 33 papers—the second highest number of papers published on the research theme, India was ranked 7th in the top countries with the highest number of citations. Iraq and Malaysia had the highest number of collaborations (LS=13), followed by Saudi Arabia and Malaysia (LS=10) and Saudi Arabia and Iraq (LS=6). Saudi Arabia and China were considered to collaborate with many countries compared to the others, with each of them collaborated with 10 and 9 countries respectively.

In the density visualization map, the country in red zone was considered to be where most papers were published in. In this study, China was the only country in the red zone, as China (documents=71) published the highest number of papers as filtered from the previous analysis restrictions. Two countries came close–India (documents=33) and Malaysia (documents=31), as both countries were placed in a yellow-reddish area of the map.

Economic feasibility

The use of metal oxide/chitosan in wastewater treatment is not only because of its good removal efficiency, but also because of its affordable price, which can save operational costs. The summary

of its utilization in cleaning organic pollutant is presented in **Figure 5**. As the by-product of the seafood industry, chitosan is easy to find at a very affordable price. [82]. On the other hand, metal oxides are quite common materials, including iron oxide, titanium oxide, and aluminum oxide. Moreover, the preparation of metal oxide also less expensive [83].

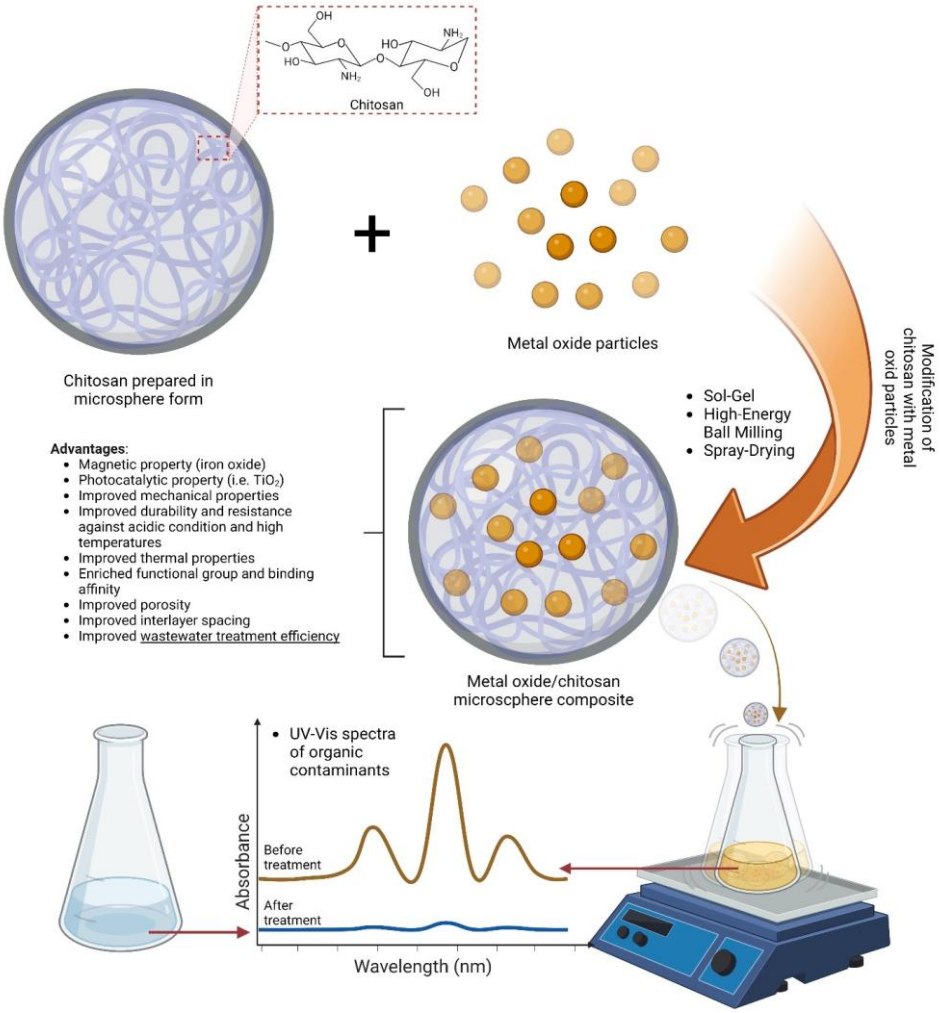

Figure 5. Schematic diagram of the review summary on the application of metal oxide/chitosan composite for organic pollutants removal. Chitosan-based matrix is used for metal-oxides embedment via sol-gel, high energy ball milling, or spray-drying. With its advantageous property, a metal oxide/chitosan composite removes the aqueous pollutants resulting in clean water.

Conclusion

Chitosan as a polymer has a good ability in wastewater removal, but it has some disadvantages such as low mechanical strength, poor acid resistance, and low recovery ability. The preparation of metal oxide/chitosan is widely studied to maximize the ability of chitosan. Many studies report that metal oxide/chitosan composites have a remarkable ability to remove wastewater. The reusability of metal oxide/chitosan composites makes them highly efficient organic wastewater removing agents. In addition, the use of metal oxide/chitosan composites is known to be affordable, because of easily available materials and less expensive methods.

Ethics approval

Not required.

Acknowledgments

None.

Competing interests

All authors declare that they have no conflicts of interest.

Funding

This study received no external funding.

Underlying data

All underlying data underlying have been presented in this article.

How to cite

Ahmad K and Chiari W. Metal oxide/chitosan composite for organic pollutants removal: A comprehensive review with bibliometric analysis. Narra X 2023; 1 (2): e91 - http://doi.org/10.52225/narrax.v1i2.91.

References

1. Ahmad K, Iqhrammullah M, Rizki DR, *et al*. Heavy Metal Contamination in Aquatic and Terrestrial Animals Resulted from Anthropogenic Activities in Indonesia: A Review. Asian J Water Environ Pollut 2022;19(4):1–8.
2. Hanafi MF, Sapawe N. A review on the water problem associate with organic pollutants derived from phenol, methyl orange, and emazol brilliant blue dyes. Mater Today: Proc 2020;31(1):A141–A150.
3. Tames F, Miglioranza KSB, Rodriguez Nunez M, *et al*. Indoor persistent organic pollutants in agricultural areas from Argentina. Indoor Air 2020;30(4):725–734.
4. Methneni N, Morales-Gonzalez JA, Jaziri A, *et al*. Persistent organic and inorganic pollutants in the effluents from the textile dyeing industries: Ecotoxicology appraisal via a battery of biotests. Environ Res 2021;196:110956.
5. Du M, Wei D, Tan Z, *et al*. Predicted no-effect concentrations for mercury species and ecological risk assessment for mercury pollution in aquatic environment. J Environ Sci 2015;28:74–80.
6. Saad AM, Abukhadra MR, Abdel-Kader Ahmed S, *et al*. Photocatalytic degradation of malachite green dye using chitosan supported ZnO and Ce-ZnO nano-flowers under visible light. J Environ Manage 2020;258:110043.
7. Beni AA, Esmaeili A. Biosorption, an efficient method for removing heavy metals from industrial effluents: A Review. Environ Technol Innov 2020;17:100503.
8. Vasseghian Y, Dragoi E-N, Almomani F, *et al*. Graphene-based membrane techniques for heavy metal removal: A critical review. Environ Technol Innov 2021;24:101863.
9. Zhang Y, Zhao M, Cheng Q, *et al*. Research progress of adsorption and removal of heavy metals by chitosan and its derivatives: A review. Chemosphere 2021;279:130927.
10. Zhang GH, Xi JB, Chen W, *et al*. Comparison in enantioseparation performance of chiral stationary phases prepared from chitosans of different sources and molecular weights. J Chromatogr A 2020;1621:461029.
11. Das A, Adak MK, Mahata N, *et al*. Wastewater treatment with the advent of TiO_2 endowed photocatalysts and their reaction kinetics with scavenger effect. J Mol Liq 2021;338:116479.
12. Davari N, Farhadian M, Nazar ARS, *et al*. Degradation of diphenhydramine by the photocatalysts of ZnO/Fe_2O_3 and TiO_2/Fe_2O_3 based on clinoptilolite: Structural and operational comparison. J Environ Chem Eng 2017;5(6):5707–5720.
13. Ikram M, Rashid M, Haider A, *et al*. A review of photocatalytic characterization, and environmental cleaning, of metal oxide nanostructured materials. Sustain Mater Technol 2021;30:e00343.
14. Boominathan T, Sivaramakrishna A. Recent advances in the synthesis, properties, and applications of modified chitosan derivatives: Challenges and opportunities. Top Curr Chem (Cham) 2021;379(3):19.
15. Rinaudo M. Chitin and chitosan: Properties and applications. Prog Polym Sci 2006; 31(7):603–632.
16. Elieh-Ali-Komi D, R HM. Chitin and chitosan: Production and application of versatile biomedical nanomaterials. Int J Adv Res 2016;4(3):411–427.
17. Yadu NVK, Raghvendra KM, Aswathy V, *et al*. Chitosan as Promising Materials for Biomedical Application: Review. Res Dev Mater Sci 2017;2(4):170–185.
18. Hajji S, Younes I, Ghorbel-Bellaaj O, *et al*. Structural differences between chitin and chitosan extracted from three different marine sources. Int J Biol Macromol 2014;65:298–306.

19. Sedaghat F, Yousefzadi M, Toiserkani H, *et al.* Bioconversion of shrimp waste Penaeus merguiensis using lactic acid fermentation: An alternative procedure for chemical extraction of chitin and chitosan. Int J Biol Macromol 2017;104(Pt A):883–888.
20. El Knidri H, El Khalfaouy R, Laajeb A, *et al.* Eco-friendly extraction and characterization of chitin and chitosan from the shrimp shell waste via microwave irradiation. Process Saf Environ Prot 2016;104:395–405.
21. Birolli WG, Delezuk JAdM, Campana-Filho SP. Ultrasound-assisted conversion of alpha-chitin into chitosan. Appl Acoustf 2016;103:239–242.
22. Fiamingo A, Delezuk JAM, Trombotto S, *et al.* Extensively deacetylated high molecular weight chitosan from the multistep ultrasound-assisted deacetylation of beta-chitin. Ultrason Sonochem 2016;32:79–85.
23. Santos VP, Maia P, de Sá Alencar N, *et al.* Recovery of chitin and chitosan from shrimp waste with microwave technique and versatile application. Arq Inst Biol 2019;86(1–7):e0982018.
24. Kundu CK, Wang X, Hou Y, *et al.* Construction of flame retardant coating on polyamide 6.6 via UV grafting of phosphorylated chitosan and sol-gel process of organo-silane. Carbohydr Polym 2018;181:833–840.
25. Li Y, Wu C, Bai Y, *et al.* Effect of glow discharge plasma on surface modification of chitosan film. Int J Biol Macromol 2019;138:340–348.
26. Alves HJ, Vieceli M, Alves C, *et al.* Chitosan Depolymerization and Nanochitosan Production Using a Single Physical Procedure. J Polym Environ 2018;26(9):3913–3923.
27. Nasrin R, Biswas S, Rashid TU, *et al.* Preparation of Chitin-PLA laminated composite for implantable application. Bioact Mater 2017;2(4):199–207.
28. Kaya M, Baran T, Karaarslan M. A new method for fast chitin extraction from shells of crab, crayfish and shrimp. Nat Prod Res 2015;29(15):1477–1480.
29. Ragab TIM, El-Bassyouni GT, Helmy WA, *et al.* Evaluation of multifunction bioactivities of extracted chitosan and their UV/ozone derivatives. J App Pharm Sci 2018;8(10):53–62.
30. Bai Q, Luo Y. Chitosan-based hydrogel beads: Preparations, modifications and applications in food and agriculture sectors–A review. Int J Biol Macromol 2020;152:437–448.
31. Chin JF, Heng ZW, Teoh HC, *et al.* Recent development of magnetic biochar crosslinked chitosan on heavy metal removal from wastewater–modification, application and mechanism. Chemosphere 2022;291:133035.
32. Ni'mah YL, Harmami H, Ulfin I, *et al.* Water-soluble chitosan preparation from marine sources. Mal J Fund Appl Sci 2019;15(2):159–163.
33. Vachoud L, Pochat-Bohatier C, Chakrabandhu Y, *et al.* Preparation and characterization of chitin hydrogels by water vapor induced gelation route. Int J Biol Macromol 2012;51(4):431–439.
34. Ali S, Ahmed S. A review on chitosan and its nanocomposites in drug delivery. Int J Biol Macromol 2018;109:409–429.
35. Peng S, Meng H, Ouyang Y, *et al.* Nanoporous Magnetic Cellulose–Chitosan Composite Microspheres: Preparation, Characterization, and Application for Cu(II) Adsorption. Ind Eng Chem Res 2014;53(6):2106–2113.
36. Zhang Y, Lin S, Qiao J, *et al.* Malic acid-enhanced chitosan hydrogel beads (mCHBs) for the removal of Cr(VI) and Cu(II) from aqueous solution. Chem Eng J 2018;353(1):225–236.
37. Lee KM, Lai CW, Ngai KS, *et al.* Recent developments of zinc oxide based photocatalyst in water treatment technology: A review. Water Res 2016;88:428–448.
38. Qi K, Yu J. Modification of ZnO-based photocatalysts for enhanced photocatalytic activity. Interface Science and Technology 2020;32:265–284.
39. Gupta SM, Tripathi M. A review of TiO_2 nanoparticles. Chin Sci Bull 2011;56(16):1639–1657.
40. Yu M, Ma Y, Liu J, *et al.* Sub-coherent growth of ZnO nanorod arrays on three-dimensional graphene framework as one-bulk high-performance photocatalyst. Appl Surf Sci 2016;390:266–272.
41. Qi K, Cheng B, Yu J, *et al.* Review on the improvement of the photocatalytic and antibacterial activities of ZnO. J Alloys and Compd 2017;727:792–820.
42. Marouzi S, Sabouri Z, Darroudi M. Greener synthesis and medical applications of metal oxide nanoparticles. Ceram Int 2021;47(14):19632–19650.
43. Hariharasuthan R, Chitradevi S, Radha K, *et al.* Characterization of NiFe2O4 (Nickel Ferrite) nanoparticles with very low magnetic saturation synthesized via co-precipitation method. Appl Phys A 2022;128(12):1045.
44. Sivakumar A, Dhas SSJ, Dhas SMB. Assessment of crystallographic and magnetic phase stabilities on MnFe2O4 nano crystalline materials at shocked conditions. Solid State Sci 2020;107:106340.

45. Yusefi M, Shameli K, Jumaat AF. Preparation and properties of magnetic iron oxide nanoparticles for biomedical applications: A brief review. J Adv Res Mater Sci 2020;75(1):10–18.
46. Vasić K, Hojnik Podrepšek G, Knez Ž, *et al*. Biodiesel production using solid acid catalysts based on metal oxides. Catalysts 2020;10(2):237.
47. Mishra P, Patnaik S, Parida K. An overview of recent progress on noble metal modified magnetic Fe_3O_4 for photocatalytic pollutant degradation and H_2 evolution. Catal Sci Technol 2019;9(4):916–941.
48. Anandhavelu S, Thambidurai S. Preparation of an ecofriendly chitosan–ZnO composite for chromium complex dye adsorption. Color Technol 2013;129(3):187–192.
49. Mostafa MH, Elsawy MA, Darwish MSA, *et al*. Microwave-Assisted preparation of Chitosan/ZnO nanocomposite and its application in dye removal. Mater Chem Phys 2020;248:122914.
50. Purohit S, Chini MK, Chakraborty T, *et al*. Rapid removal of arsenic from water using metal oxide doped recyclable cross-linked chitosan cryogel. SN Appl Sci 2020;2(4):768.
51. Makeswari M, Saraswathi P. Photo catalytic degradation of methylene blue and methyl orange from aqueous solution using solar light onto chitosan bi-metal oxide composite. SN Appl Sci 2020;2(3):336.
52. Mohamed HS, Soliman NK, Moustafa AF, *et al*. Nano metal oxide impregnated Chitosan-4-nitroacetophenone for industrial dye removal. Int J Environ Anal Chem 2019;101(13):1850–1877.
53. Rani M, Rachna, Shanker U. Metal oxide-chitosan based nanocomposites for efficient degradation of carcinogenic PAHs. J Environ Chem Eng 2020;8(3):103810.
54. Chaudhary M, Rawat S, Jain N, *et al*. Chitosan-Fe-Al-Mn metal oxyhydroxides composite as highly efficient fluoride scavenger for aqueous medium. Carbohydr Polym 2019;216:140-148.
55. Lu J, Li B, Li W, et al. Nano iron oxides impregnated chitosan beads towards aqueous Cr (VI) elimination: Components optimization and performance evaluation. Colloids Surf A: Physicochem Eng 2021;625:126902.
56. Butto N, Cotrina Vera N, Díaz-Soler F, *et a*l. Effect of Chitosan Electrospun Fiber Mesh as Template on the Crystallization of Calcium Oxalate. Crystals 2020;10(6):453.
57. Geerdink RB, van den Hurk RS, Epema OJ, *et al*. Chemical oxygen demand: Historical perspectives and future challenges. Anal Chim Acta 2017;961:1–11.
58. Zhao Y, Tao C, Xiao G, *et al*. Controlled synthesis and wastewater treatment of Ag2O/TiO2 modified chitosan-based photocatalytic film. RSC Adv 2017;7(18):11211–11221.
59. González JA, Villanueva ME, Piehl LL, *et al*. Development of a chitin/graphene oxide hybrid composite for the removal of pollutant dyes: Adsorption and desorption study. Chem Eng J 2015;280:41–48.
60. Sirajudheen P, Karthikeyan P, Ramkumar K, *et al*. Effective removal of organic pollutants by adsorption onto chitosan supported graphene oxide-hydroxyapatite composite: A novel reusable adsorbent. J Mol Liq 2020;318:114200.
61. Al-Taweel SS, Saud HR, Kadhum AAH, *et al*. The influence of titanium dioxide nanofiller ratio on morphology and surface properties of TiO_2/chitosan nanocomposite. Results Phys 2019;13:102296.
62. Senthil Kumar P, Selvakumar M, Babu SG, *et al*. Novel CuO/chitosan nanocomposite thin film: Facile hand-picking recoverable, efficient and reusable heterogeneous photocatalyst. RSC Adv 2015;5(71):57493–57501.
63. Siddeeg SM, Tahoon MA, Mnif W, *et al*. Iron oxide/chitosan magnetic nanocomposite immobilized manganese peroxidase for decolorization of textile wastewater. Processes 2019;8(1):5.
64. Le TTN, Le VT, Dao MU, *et al*. Preparation of magnetic graphene oxide/chitosan composite beads for effective removal of heavy metals and dyes from aqueous solutions. Che Eng Comm 2019;206(10):1337–1352.
65. Fan L, Luo C, Li X, *et al*. Fabrication of novel magnetic chitosan grafted with graphene oxide to enhance adsorption properties for methyl blue. J Hazard Mater 2012;215–216:272–279.
66. Cinar S, Kaynar UH, Aydemir T, *et al*. An efficient removal of RB5 from aqueous solution by adsorption onto nano-ZnO/Chitosan composite beads. Int J Biol Macromol 2017;96:459–465.
67. Arafat A, Samad SA, Huq D, *et al*. Textile Dye Removal from wastewater effluents using chitosan-ZnO nanocomposite. J Text Sci Eng 2015;5(3):1000200.
68. Khan H, Khalil AK, Khan A, *et al*. Photocatalytic degradation of bromophenol blue in aqueous medium using chitosan conjugated magnetic nanoparticles. Korean J Chem Eng 2016;33:2802–2807.
69. Cuana R, Panre AM, Istiqomah NI, *et al*. Green synthesis of Fe_3O_4/Chitosan nanoparticles utilizing *Moringa oleifera* extracts and their surface plasmon resonance properties. ECS J Solid State Sci Technol 2022;11(8):083015.
70. Li G-y, Jiang Y-r, Huang K-l, *et al*. Preparation and properties of magnetic Fe_3O_4–chitosan nanoparticles. J Alloys Compd 2008;466(1):451–456.

71. Kumar PS, Selvakumar M, Babu SG, *et al*. Novel CuO/chitosan nanocomposite thin film: facile hand-picking recoverable, efficient and reusable heterogeneous photocatalyst. RSC Adv 2015;5(71):57493–57501.
72. Das L, Das P, Bhowal A, *et al*. Synthesis of hybrid hydrogel nano-polymer composite using Graphene oxide, Chitosan and PVA and its application in wastewater treatment. Environ Technol Innov 2020;18:100664.
73. Singh N, Riyajuddin S, Ghosh K, *et al*. Chitosan-graphene oxide hydrogels with embedded magnetic iron oxide nanoparticles for dye removal. ACS Appl Nano Mate 2019;2(11):7379–7392.
74. González-López ME, Robledo-Ortíz JR, Rodrigue D, *et al*. Highly porous lignin composites for dye removal in batch and continuous-flow systems. Mater Lett 2020;263:127289.
75. Leudjo Taka A, Klink MJ, Yangkou Mbianda X, *et al*. Chitosan nanocomposites for water treatment by fixed-bed continuous flow column adsorption: A review. Carbohydr Polym 2021;255:117398.
76. Qi C, Zhao L, Lin Y, *et al*. Graphene oxide/chitosan sponge as a novel filtering material for the removal of dye from water. J Colloid Interface Sci 2018;517:18–27.
77. Bai B, Xu X, Li C, *et al*. Magnetic Fe_3O_4@Chitosan carbon microbeads: removal of doxycycline from aqueous solutions through a fixed bed via sequential adsorption and heterogeneous fenton-like regeneration. J Nanomater 2018;2018:1–14.
78. van Eck NJ, Waltman L. Software survey: VOSviewer, a computer program for bibliometric mapping. Scientometrics 2010;84(2):523–538.
79. Chiari W, Damayanti R, Harapan H, *et al*. Trend of polymer research related to COVID-19 Pandemic: Bibliometric analysis. Polymers 2022;14(16):3297.
80. Iqhrammullah M, Fahrina A, Chiari W, *et al*. Laccase Immobilization Using Polymeric Supports for Wastewater Treatment: A Critical Review. Macromol Chem Phys 2023;224(9):2200461.
81. Puspita K, Chiari W, Abdulmadjid SN, *et al*. Four Decades of Laccase Research for Wastewater Treatment: Insights from Bibliometric Analysis. Int J Environ Res Public Health 2022;20(1):308.
82. Kou SG, Peters LM, Mucalo MR. Chitosan: A review of sources and preparation methods. Int J Biol Macromol 2021;169:85–94.
83. Gautam S, Agrawal H, Thakur M, *et al*. Metal oxides and metal organic frameworks for the photocatalytic degradation: A review. J Env Chem Eng 2020;8(3):103726.
84. Meramo-Hurtado SI, Gonzalez-Delgado AD. Application of techno-economic and sensitivity analyses as decision-making tools for assessing emerging large-scale technologies for production of chitosan-based adsorbents. ACS Omega 2020;5(28):17601–17610.
85. Mpongwana N, Rathilal S. A review of the techno-economic feasibility of nanoparticle application for wastewater treatment. Water 2022;14(10):1550.